



**WESTERN REGION TECHNICAL ATTACHMENT
NO. 99-22
OCTOBER 12, 1999**

**KYUX WSR-88D RAINFALL ESTIMATES DURING
TROPICAL STORM NORA**

Naeemah Cushmeer - NWSO Las Vegas, NV

Introduction

Tropical Storm Nora entered the far southwest United States, near the California/Arizona border, during the afternoon of 25 September 1997 (Fig. 1 shows the storm track). Nora produced rainfall that nearly equaled or surpassed the average annual amount for some desert locations in southwest Arizona and southeast California. The 12.01 inches (~305 mm) of rain recorded by an automated gauge (Harquahala Mountain) in southwest Arizona unofficially established a new record 24-hour rainfall amount for the state (The official record is 11.40 inches or ~300 mm).

Background

Prior to Tropical Storm Nora's landfall, the National Weather Service Forecast Office (NWSFO) in Phoenix, Arizona decided that the Rosenfeld tropical Z-R ($Z=250R^{1.2}$) relationship would be utilized during the event on KYUX, the Weather Surveillance Radar-1988, Doppler (WSR-88D) located south of Yuma, Arizona. In coordination with adjacent National Weather Service Offices (NWSOs) and the Colorado Basin River Forecast Center (CBRFC), NWSFO Phoenix switched to the Rosenfeld tropical Z-R relationship about eighteen hours prior to the storm's passage. The decision to change the Z-R relationship from the default ($Z=300R^{1.4}$) at that time was based on the observation that the WSR-88D was significantly underestimating rainfall from bands of heavy precipitation occurring in advance of Nora. The Maximum Precipitation Rate Allowed (MXPRA) was also changed from the default value of 103.8 mm/hr (~4 in/hr) to 150 mm/hr (~6 in/hr). The radar was operating in Volume Coverage Pattern (VCP) 21 during the entire event.

The default Z-R relationship was employed on Phoenix's (KIWA) WSR-88D during the entire event. The primary reason for this was that the tropical air mass was expected to (and did) remain mostly outside KIWA's radar umbrella. Table 1 shows the difference between the Rosenfeld and default Z-R relationships for various reflectivity values. A scatter plot depicting the observed versus the radar derived amounts for both KIWA and KYUX can be seen in Fig. 2 (Note: The line represents perfect agreement). A detailed comparison between the two radars is beyond the scope of this paper.

Figure 3 is an isohyetal analysis of the observed rainfall amounts, associated with Nora, that fell during the period ending 0600 UTC 26th September (The rain gauge network within the radar umbrella is rather sparse). KYUX storm total precipitation for the time period is presented in Fig. 4. In general, KYUX underestimated rainfall amounts, especially within 30 NM of the WSR-88D, by as much as a factor of 12! This paper will attempt to answer this question: Why did KYUX underestimate rainfall amounts for this tropical event?

Sources of Errors Associated with Underestimated Rainfall Amounts

The following are factors that may cause the radar to underestimate precipitation.

1. Partial Beam Filling
2. Attenuation (from a wet radome, rain, or atmospheric gases)
3. Incorrect hardware calibration
4. Forced clutter filtering (in areas of no clutter)
5. Variation in drop-size distribution
6. Strong wind below cloud base
7. Coalescence below radar beam
8. Vertical air motion

Incorrect hardware calibration (3) and forced clutter filtering in areas of no clutter (4) probably did not affect the radar estimates. The Delta System Calibration (Delta Sys Cal) was within tolerance (greater than -2dB and less than 2 dB). Recall that the Delta Sys Cal value is used as a correction factor (for noise in the Z, reflectivity, value) for each volume scan. This correction is applied to ensure the radar is operating within tolerance. During the event no forced clutter filtering was applied within the radar domain (Note: Clutter contamination presumably led to rainfall overestimation over Baja California).

It was unlikely that strong wind below cloud base (6) was a factor in this case. Strong winds, on the order of 20 to 30 knots (10 to 15 ms⁻¹), did occur in association with Nora on the 25th; however, the strong winds occurred across a

fairly widespread area. As a consequence, the pattern of heavy rainfall is inferred to have been uniformly dispersed by the wind field. Precipitation with the storm system was fairly widespread (and of varying intensities); therefore, partial beam filling (1) was not a major factor.

Radars measure returned power not drop-size distribution. Reflectivity, Z , is dependent on the drop-size distribution and the sixth power of the drop diameter. Rainfall, R is dependent on the drop size distribution, fall velocity of the drops, and the third power of the drop diameter. Consequently, different reflectivity values could be associated with identical rainfall rates; conversely, different rainfall rates could be observed in areas of identical reflectivity. Due to the tropical character of the event, it was likely that a breakup of large drops into numerous small ones had occurred. This variation in drop size distribution from the assumed Z - R relationship would lead to underestimation of rainfall amounts by the WSR-88D.

Collision coalescence (numerous small raindrops adhering together as they fall) below the radar beam (7), a common occurrence during tropical events, may have also contributed to the underestimation of rainfall. During collision coalescence, the higher reflectivity values tend to occur in the lower portion of the storm cloud. This could result in the beam overshooting the higher reflectivity values, especially at far distances from the radar. Analysis of the lowest four base reflectivity slices (not presented) showed that the highest reflectivity values were mostly below 2.4°(the lower portion of the storm cloud) during the event.

Underestimation of the precipitation could be attributed to attenuation of the returned signal from wetting of the radome and heavy rainfall. Baeck and Smith (1998) presented a case in which heavy rain falling on the radome led to significant precipitation underestimation by the Chicago WSR-88D.

Vertical air motion (updrafts and downdrafts) within a storm cloud (8) is another potential source of error. In updraft regions, the total water mass rates are overestimated whereas in regions of downdrafts the converse is true (Doviak and Zrnic, 1984). The following equation describes error in water mass per unit time (Doviak and Zrnic, 1984):

$$\text{error} = \iint w(\mathbf{r})M(\mathbf{r})dA,$$

where w is the vertical air velocity, M is the liquid water content, \mathbf{r} is the vector range, and A is the catchment area. As w increases (either upward or downward), the errors grow and become more dependent on rainfall rates (Doviak and Zrnic, 1984). Figure 5 shows a reconstructed Skew-T sounding for Yuma (1200 UTC, 25 September) using data from the ETA model (the actual upper air information for Yuma was unavailable). As shown by the sounding, there was relatively little

positive area (716 Jkg^{-1}); therefore, vertical air motion is presumed to have had minor impact on the radar rainfall estimates. Vertical air motion would be more of a source of error with deep convection associated with intense thunderstorms (larger values of w).

WSR-88D Precipitation Processing System

Base reflectivity data from the lowest four elevation slices is used in the precipitation processing algorithm. The data is subjected to five quality control checks to correct for the following: radar beam blockage, spurious noise, reflectivity outliers, ground returns, and change in beam height with range.

Rainfall would be underestimated if there were no correction for physical blockage of the radar beam. A predefined dBZ value is added for beam obstructions less than or equal to 60%. If the blockage is greater than 60%, the algorithm checks to see how much of the sample volume is obstructed. If the blockage is 2° or less in azimuth, the average value of the range bins next to the obstruction is assigned to the blocked bins. If the blockage is greater than 2° , then the value of the next highest elevation slice is assigned to the obstructed sector. Figure 6 shows the terrain heights for KYUX.

A sectorized hybrid scan is used to correct for changes in beam height with range. In the absence of significant beam obstruction, reflectivity data from higher elevation slices (3.4° and 2.4°) is used at near ranges (within 19 NM or 35 km) while lower elevation angles (0.5° or 1.5°) are used at farther ranges (beyond 27 NM) from the radar. At mid ranges (19 NM to 27 NM) from the radar, data is taken from the 1.5° slice. The purpose of the sectorized hybrid scan is to attempt to sample a near uniform height above the ground. If the beam does not clear an obstacle by 500 feet (150 m) and the beam is more than 50% blocked beyond the obstruction, then data from the next (higher) slice is used. The hybrid scan elevations for KYUX are displayed in Fig. 7.

Echo tops during the period of interest averaged about 25,000 feet (7.6 km), with peak reflectivity values averaging about 35 dBZ (the higher reflectivity values occurred mostly below the 2.4° slice). Table 2 presents the range from the radar and the probable beam height for each gauge site.¹ Inadequate sampling of the storm cloud could explain why amounts were underestimated. At greater distances from the radar, the beam was likely overshooting the storm core. For example, the

¹ Level II data was unavailable for this event due to a hardware malfunction.

gauge west of Arlington is 86 NM (159 km) from the radar. At this distance, the beam was probably near 17,000 ft (5 km); therefore, input from reflectivity data at this height was from near the top of the cloud. At ranges close to the radar, the beam was likely undershooting the storm core. The gauge site at Yuma is only 9 NM (17 km) from the radar. Reflectivity data from the 3.4° elevation slice was likely used at this range. This places the beam a mere 3,500 feet (1 km) above the ground.

Conclusion/Recommendation

A map of the radar bias is presented in Fig. 8. The bias was computed as the WSR-88D derived rainfall estimate divided by the observed rainfall (R/O). For simplicity, the midpoint of the precipitation data level was used as the radar rainfall estimate. Based on the pattern of the bias, several assumptions could be made. The region north and northeast of the radar, where the biases were less than 0.5, was located in the tropical air mass (The heaviest rainfall fell mostly in the northeast quadrant of Nora's center). In this area, where breakup of large drops into a significant number of small ones likely occurred, the drop-size distribution deviated from that assumed by the Z-R equation. The regions, where the bias exceeded one (rainfall overestimated), appear to define where the air mass was less tropical in character. The default relationship, if it were employed, could have provided better rainfall estimates for these regions. To the west of the radar, the bias approached perfect agreement (1.0). It was presumed that the drop-size distribution in this zone came close to the Z-R assumption. However, farther northwest of the radar (beyond 100 NM) the biases dropped to less than 0.5. Range effects and variation in drop-size distribution due to orographic enhancement were probably responsible for the underestimates in this region. Variations in drop-size distribution seemed to have been a major source of error in KYUX's rainfall estimates; therefore, it would appear that neither the Rosenfeld tropical or default Z-R relationship was valid for this particular event.

This case presents a strong need for the implementation of Stage II precipitation processing. In complex situations such as this, no one Z-R relationship could apply to the entire radar domain. Although a mean field bias adjustment would not have taken into account the spatial variability of the bias, it still would have resulted in substantial improvement of the rainfall estimates for this event.

Polarimetric technology, if implemented by the National Weather Service in the future, has potential to significantly improve WSR-88D radar rainfall estimates (Fulton, et al. 1998; Baeck and Smith, 1998). The addition of vertical polarization measurements on the WSR-88Ds would provide the capability of inferring drop-size and precipitation type (Fulton et al. 1998).

Acknowledgments

The author wishes to thank Steve Waters and Julie Riemenschneider (Maricopa County Flood Control District) for providing the ALERT rain gauge data and Jonathan J. Gurley (CIMMS, University of Oklahoma) for providing the radar beam heights as a function of range for KYUX.

References

- Baeck, M.L., and J.A. Smith, 1998: Rainfall Estimation by the WSR-88D for Heavy Rainfall Events. *Wea. and Forecasting*, **13(2)**, 432, 435.
- Belville, J.D., 1997: *Recommended Parameter Changes to Improve WSR-88D Tropical Rainfall Estimates*. WSR-88D Operational Support Facility Memorandum, 4/22/97.
- Doviak, R.J., and D.S. Zrnic, 1984: *Doppler Radar and Weather Observations*, Academic Press, Inc., Orlando, 458 pp.
- Fulton, R.A., J.P. Breidenbach, D. Seo, D.A. Miller, T. O'Bannon, 1998: The WSR-88D Rainfall Algorithm. *Wea. and Forecasting*, **13(2)**, 380, 391.
- Rappaport, E.N., 1997: National Hurricane Center Preliminary Report, Hurricane Nora, 10/18/97.
- WSR-88D Operations Course, 1977: Topics 3 and 8, Operational Training Branch, Operational Support Facility, 3-39 through 3-66 and 8-173 through 8-208.

WSR-88D Estimated Rainfall Rates

WSR-88D Default Z-R Relationship Versus The Rosenfeld Tropical Relationship

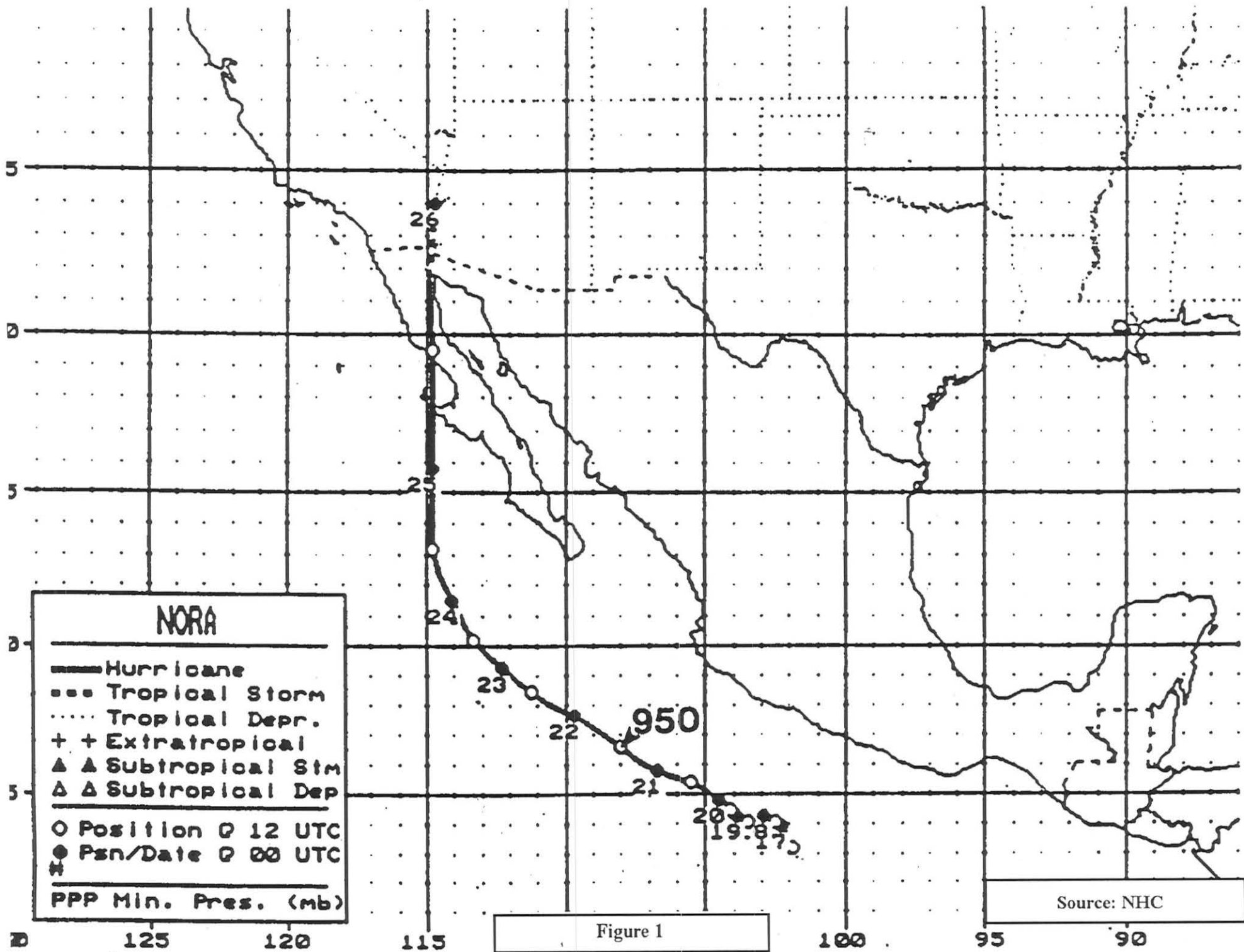
<u>Reflectivity</u>	<u>WSR-88D default ($Z=300R^{1.4}$)</u>	<u>Rosenfeld tropical ($Z=250R^{1.2}$)</u>
20 dBZ	0.02 in/hr	0.02 in/hr
25 dBZ	0.04 in/hr	0.05 in/hr
30 dBZ	0.09 in/hr	0.12 in/hr
35 dBZ	0.21 in/hr	0.33 in/hr
40 dBZ	0.48 in/hr	0.85 in/hr
45 dBZ	1.10 in/hr	2.22 in/hr
50 dBZ	2.50 in/hr	5.80 in/hr
55 dBZ	5.68 in/hr	15.14 in/hr

Table 1

GAGE SITE	Range from RDA	Probable Beam Height	WSR-88D Estimate (in)	Observed Rainfall (in)
Aguila 11 S (AZ)	108 NM (200 km)	3,100 ft (4 km)	0.80	2.02
Arlington 26 W (AZ)	86 NM (159 km)	17,100 ft (5 km)	0.80	2.45
Blythe (CA)	68 NM (126 km)	9,800 ft (2 km)	0.45	2.03
Bouse (AZ)	92 NM (170 km)	11,400 ft (3 km)	0.45	0.88
Borrego Springs (CA)	98 NM (181 km)	12,500 ft (4 km)	1.25	1.79
Buckeye 5 N (AZ)	118 NM (218 km)	14,800 ft (5 km)	0.45	0.16
Buckeye 11 NW (AZ)	102 NM (189 km)	11,800 ft (4 km)	0.15	0.40
Gila Bend 23 W (AZ)	84 NM (155 km)	17,400 ft (5 km)	0.80	1.31
Harquahala Mt (AZ)	103 NM (191 km)	12,100 ft (4 km)	0.80	9.45
Hassayampa 2 NW (AZ)	110 NM (204 km)	13,400 ft (4 km)	0.80	0.40
Imperial (CA)	50 NM (93 km)	10,100 ft (3 km)	0.80	0.85
Parker (AZ)	101 NM (187 km)	12,100 ft (4 km)	0.80	1.61
Salome 26 SE (AZ)	98 NM (181 KM)	11,500 ft (4 km)	0.80	2.01
Smith Peak (AZ)	115 NM (213 km)	14,800 ft (5 km)	1.25	2.17
Tacna (AZ)	38 NM (70 km)	6,900 ft (2 km)	0.45	1.38
Thermal (CA)	102 NM (189 km)	12,100 ft (4 km)	1.75	1.99
Tiger Wash Fan (AZ)	97 NM (180 km)	11,500 ft (4 km)	0.45	2.12
Tonopah 7 WSW (AZ)	99 NM (183 km)	11,800 ft (4 km)	0.80	1.50
Tonopah 10 WNW (AZ)	101 NM (187 km)	12,800 ft (4 km)	0.80	1.03
Twentynine Palms (CA)	121 NM (224 km)	16,400 ft (5 km)	0.80	3.07
White Tanks East Pk (AZ)	124 NM (230 km)	16,400 ft (5 km)	0.15	0.48
Yuma (AZ)	9 NM (17 km)	3,500 ft (1 km)	0.80	3.83

SUM: 16.40 42.93
AVG: 0.75 1.95

Table 2



WSR-88D Rainfall Estimates Versus Observed Rainfall

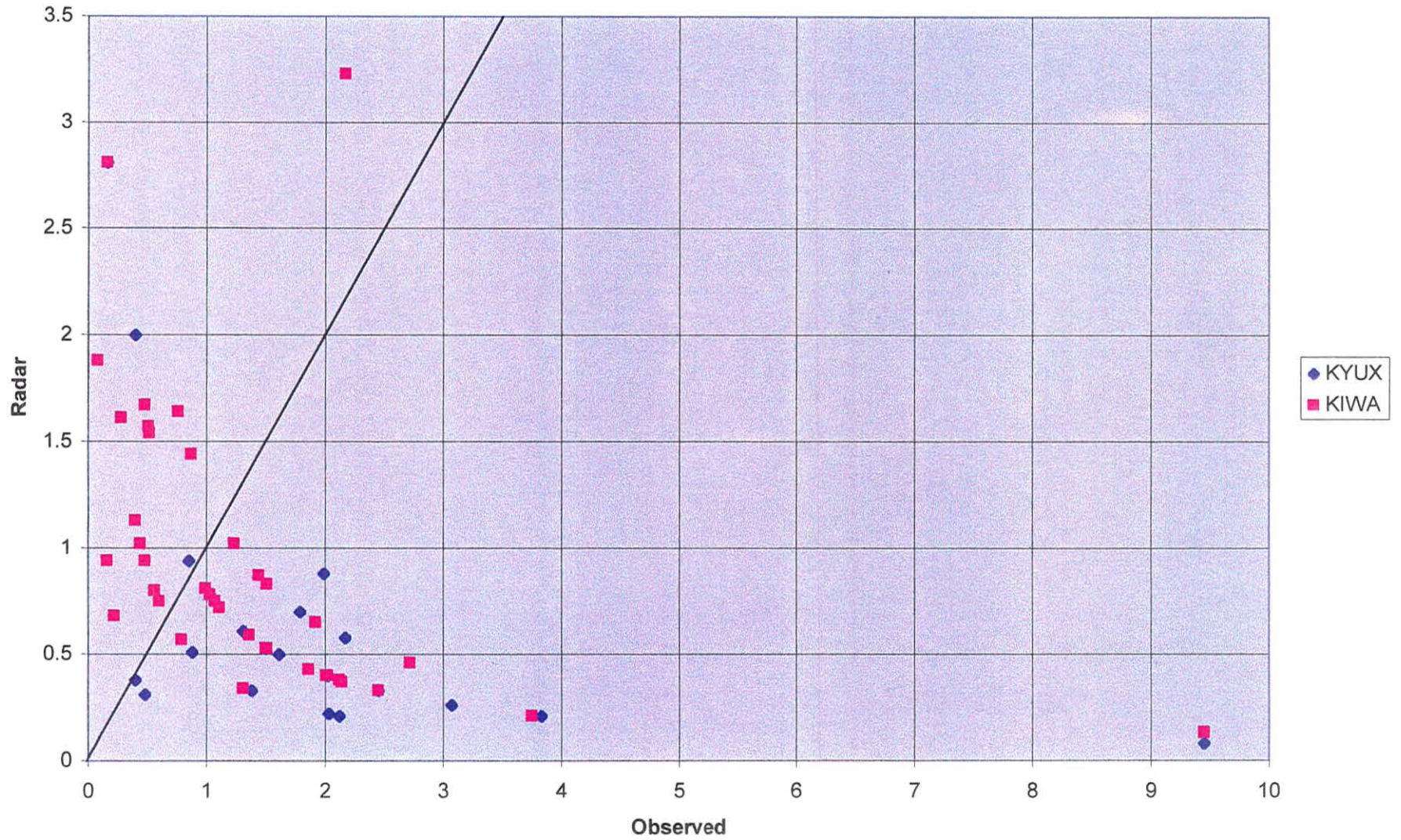
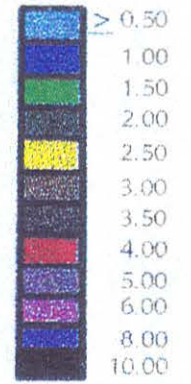


Figure 2

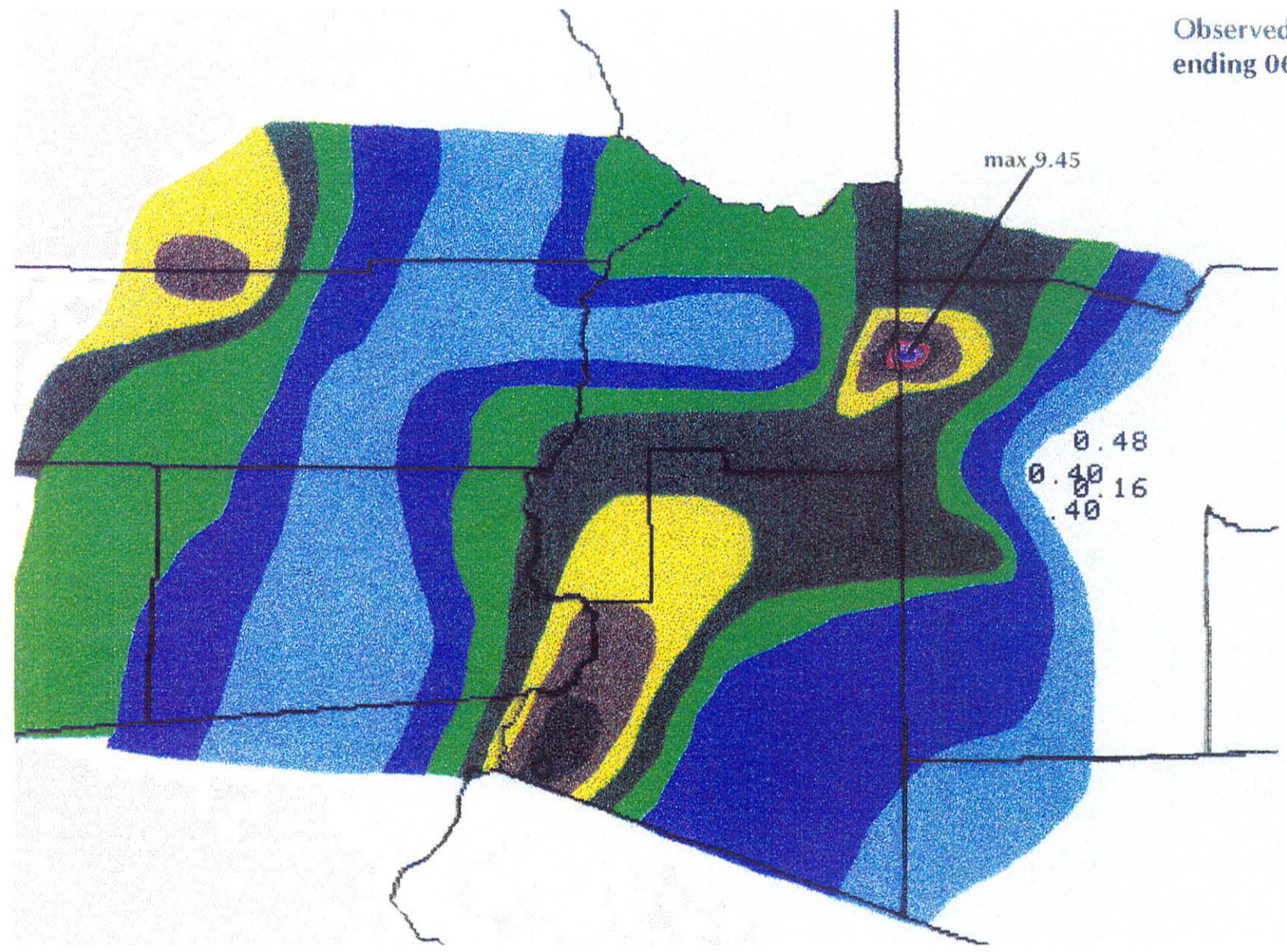
Observed Storm Total Rainfall (in)
ending 0600 UTC 26 SEP 1997



max 9.45

0.48
0.40
0.16
.40

Figure 3



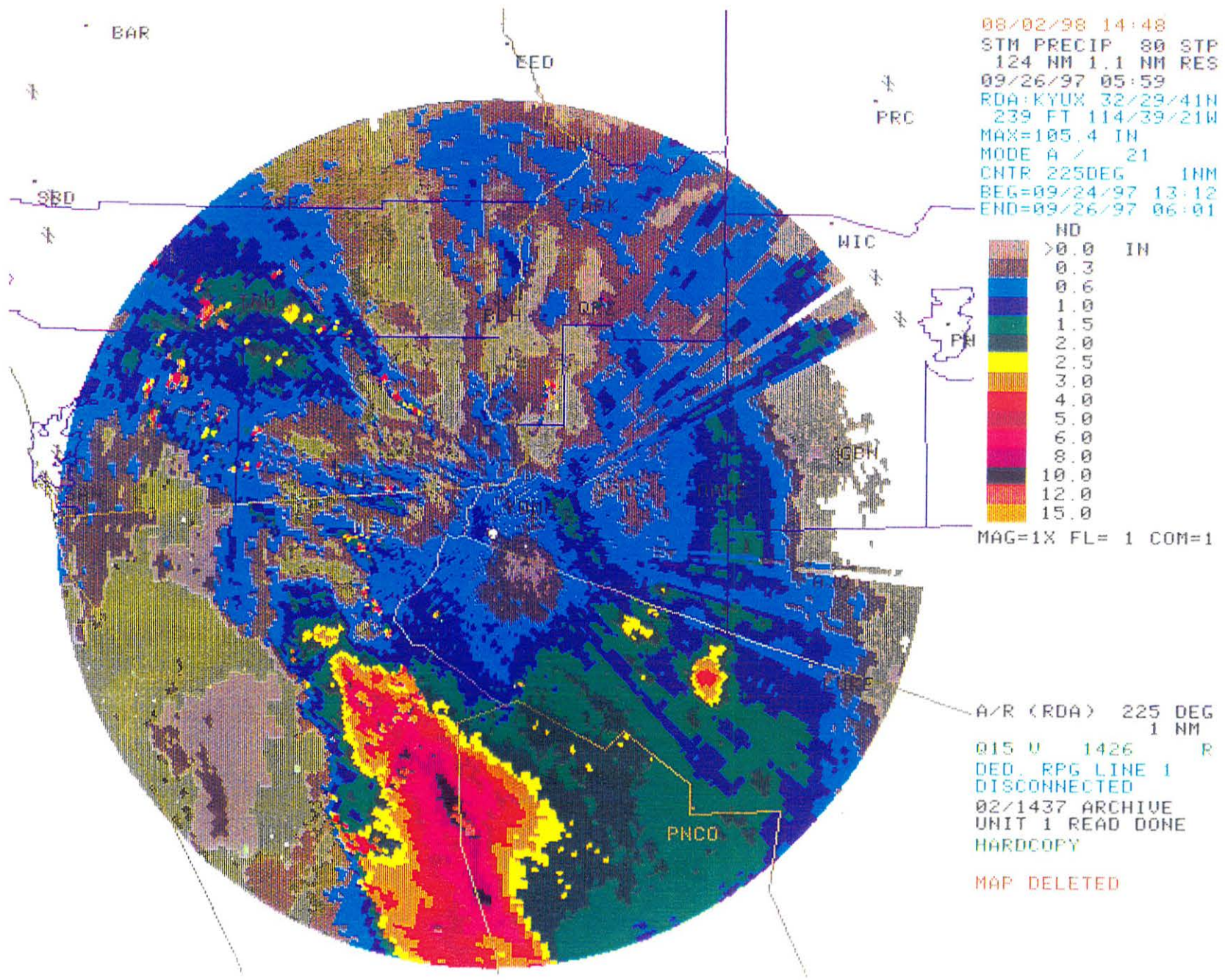


Figure 4

LI 4.3
 TT 43.0
 TEI 16.7
 K 2.5
 SWEAT 2.9
 CAP 0.8

CURSOR DATA
 1050mb
 -999m -999'
 $\theta = 228$ $T_s = 24F$
 $w = 0.1$
 -41.5C -43F

RAOB DATA
 P 992
 T 24.0
 Td 23.0
 Tdd 1.0
 Wind .. 20/09

PARCEL DATA
 B+ 716
 B- 155
 LPL .. 950mb
 EL .. 26400ft
 MPL .. -999ft
 LCL .. 915ft
 FZL .. 12749ft
 WBZ .. 11637ft
 PW ... 2.22in

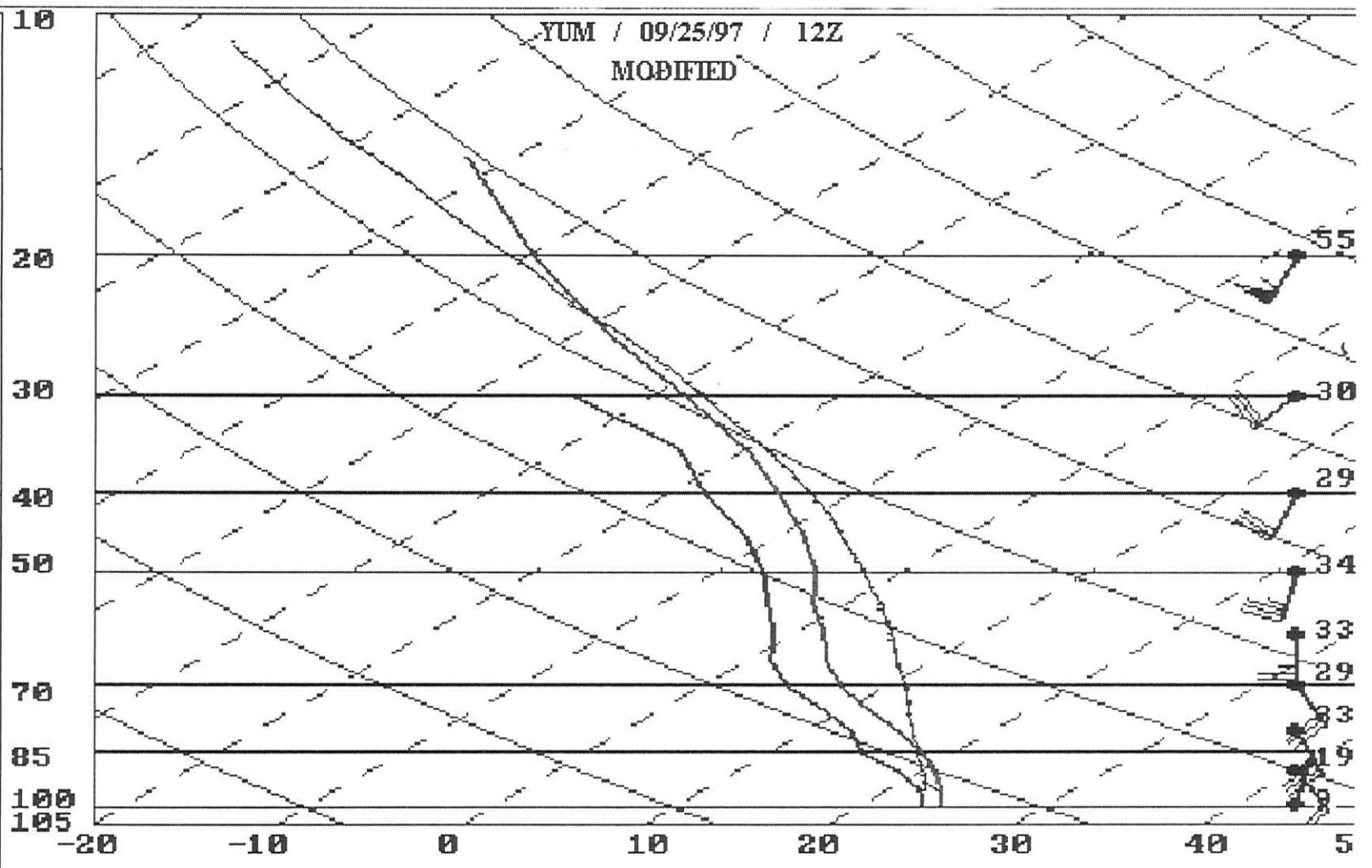
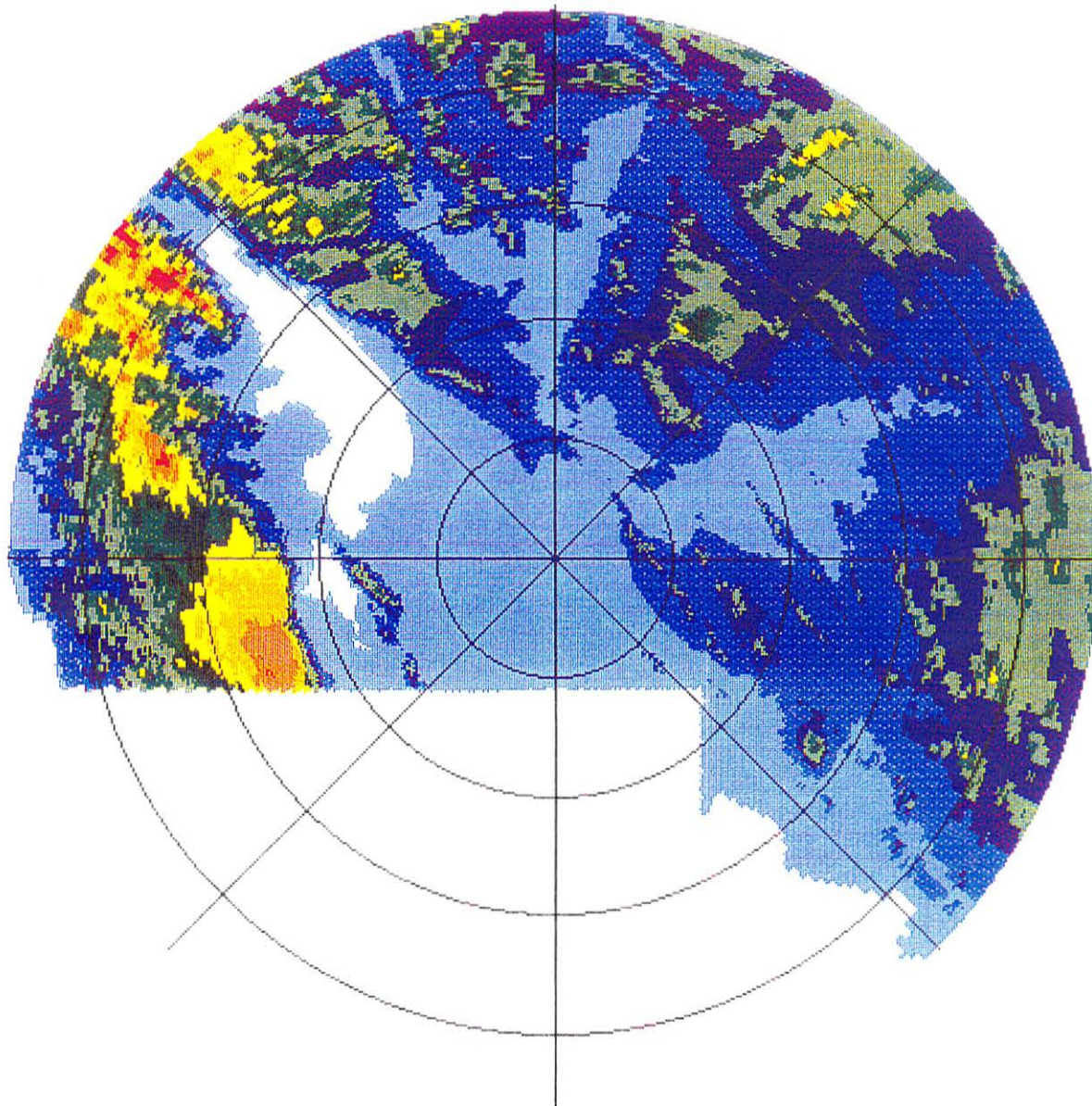


Figure 5



TERRAIN HEIGHTS
 RADAR ID: KYUX
 RDA HGT: 40 M
 MIN HGT: 1 M
 MAX HGT: 2600 M

- | | |
|-------------|-------------|
| NO DATA | NO DATA |
| 1 METER | 1 METER |
| 200 METERS | 200 METERS |
| 400 METERS | 400 METERS |
| 600 METERS | 600 METERS |
| 800 METERS | 800 METERS |
| 1000 METERS | 1000 METERS |
| 1200 METERS | 1200 METERS |
| 1400 METERS | 1400 METERS |
| 1600 METERS | 1600 METERS |
| 1800 METERS | 1800 METERS |
| 2000 METERS | 2000 METERS |
| 2200 METERS | 2200 METERS |
| 2400 METERS | 2400 METERS |
| 2600 METERS | 2600 METERS |
| 2800 METERS | 2800 METERS |

MAX RANGE 230 KM
 RANGE RINGS 50 KM

Figure 6

HYBRID SCAN ELEUS
RADAR ID: KYUX

ELEV 1 OR 2
ELEV 3 ONLY
ELEV 3 ONLY
ELEV 4 ONLY

MAX RANGE 230 KM
RANGE RINGS 30 KM

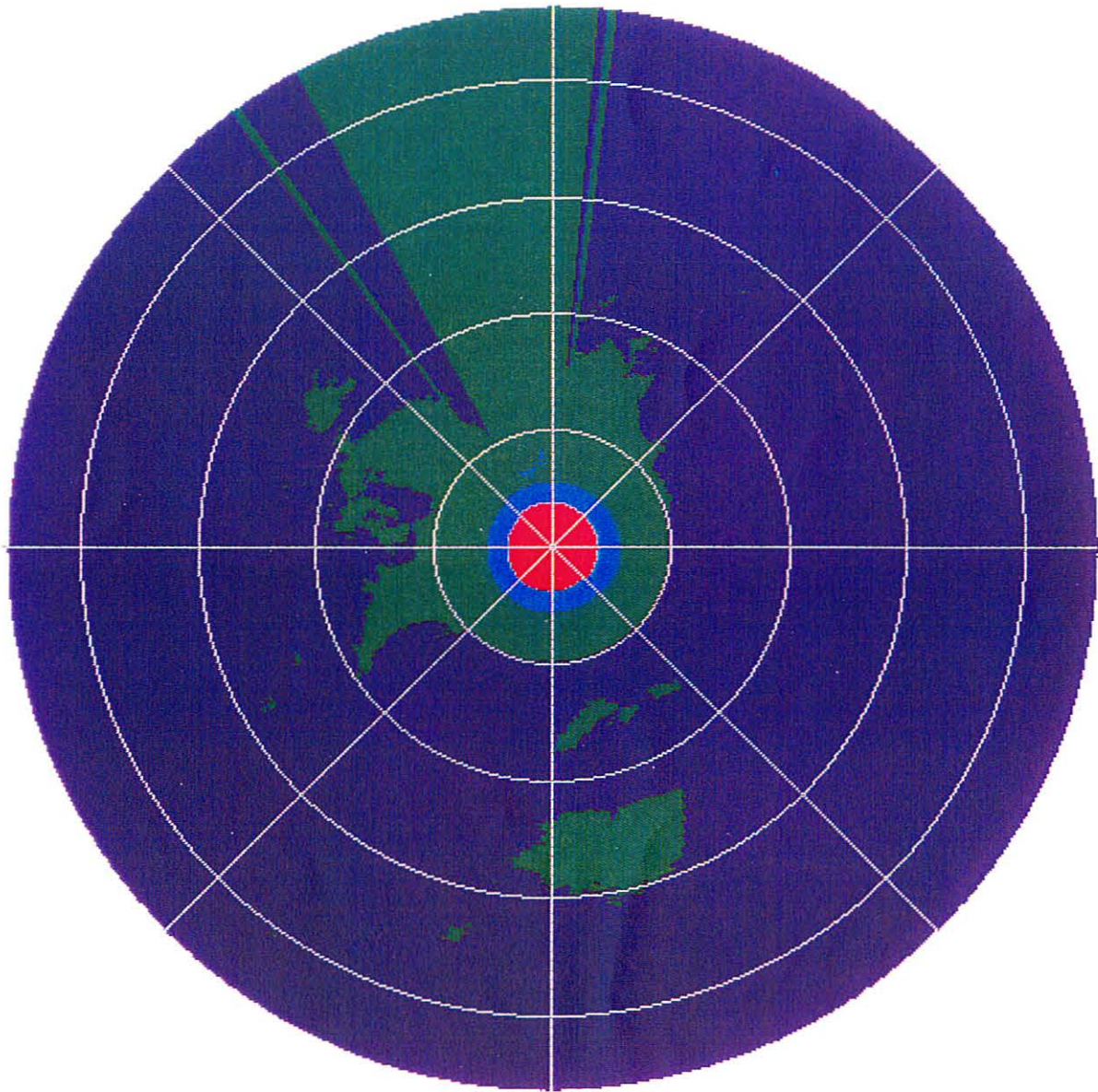


Figure 7

KYUX WSR-88D Rainfall Bias

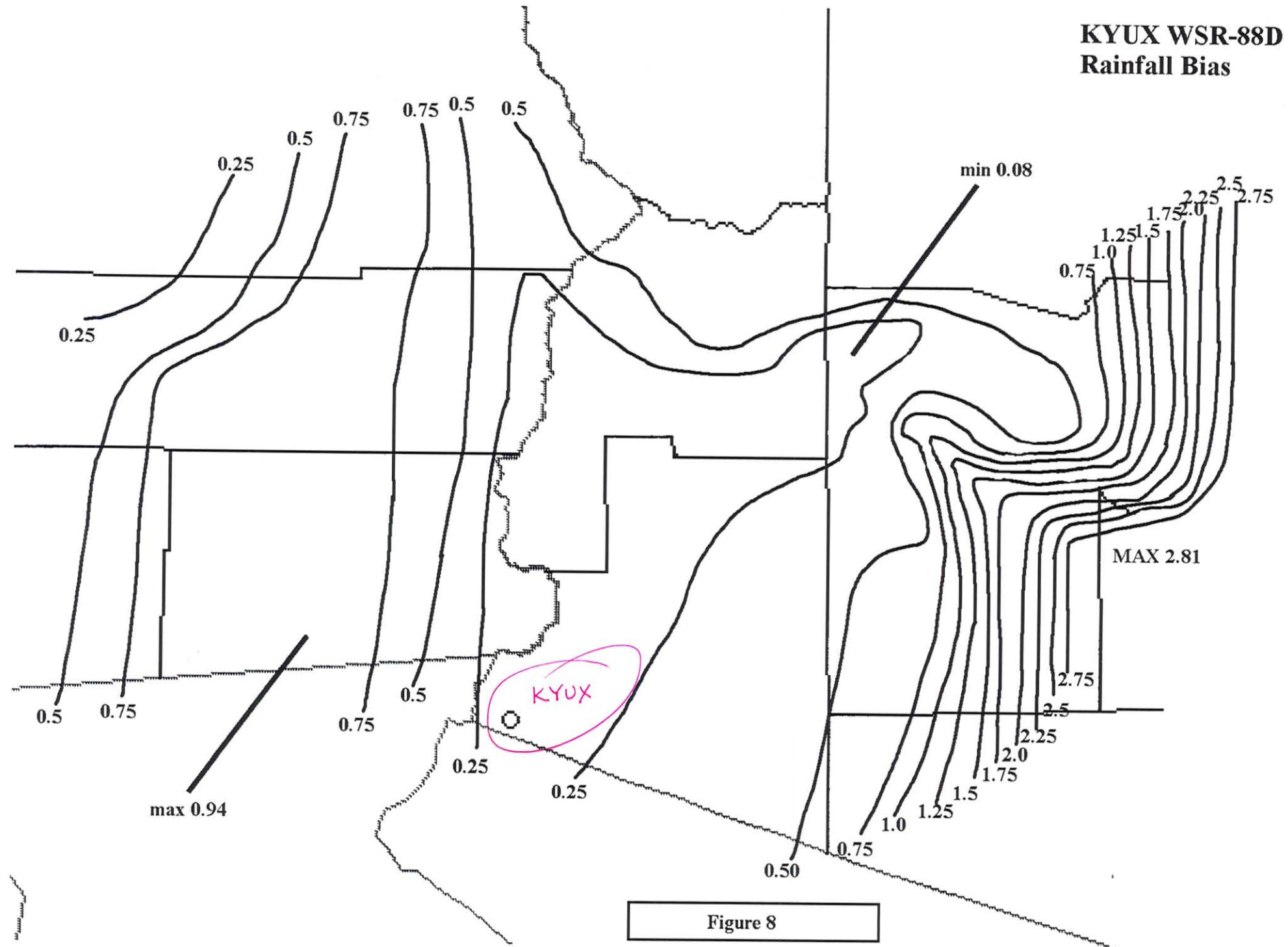


Figure 8